

Article

Expression of Long Non-Coding RNAs by Human Retinal Müller Glial Cells Infected with Clonal and Exotic Virulent *Toxoplasma gondii*

Elise Rochet, Binoy Appukuttan, Yuefang Ma, Liam M. Ashander and Justine R. Smith * 

Flinders University College of Medicine & Public Health, Adelaide, SA 5042, Australia; rochet.elise@gmail.com (E.R.); binoy.appukuttan@flinders.edu.au (B.A.); yuefang.ma@flinders.edu.au (Y.M.); liam.ashander@flinders.edu.au (L.M.A.)

* Correspondence: justine.smith@flinders.edu.au; Tel.: +61-8-8204-4300

Received: 15 August 2019; Accepted: 18 September 2019; Published: 20 September 2019



Abstract: Retinal infection with *Toxoplasma gondii*—ocular toxoplasmosis—is a common cause of vision impairment worldwide. Pathology combines parasite-induced retinal cell death and reactive intraocular inflammation. Müller glial cells, which represent the supporting cell population of the retina, are relatively susceptible to infection with *T. gondii*. We investigated expression of long non-coding RNAs (lncRNAs) with immunologic regulatory activity in Müller cells infected with virulent *T. gondii* strains—GT1 (haplogroup 1, type I) and GPHT (haplogroup 6). We first confirmed expression of 33 lncRNA in primary cell isolates. MIO-M1 human retinal Müller cell monolayers were infected with *T. gondii* tachyzoites (multiplicity of infection = 5) and harvested at 4, 12, 24, and 36 h post-infection, with infection being tracked by the expression of parasite surface antigen 1 (SAG1). Significant fold-changes were observed for 31 lncRNAs at one or more time intervals. Similar changes between strains were measured for BANC1, CYTOR, FOXD3-AS1, GAS5, GSTT1-AS1, LINC-ROR, LUCAT1, MALAT1, MIR22HG, MIR143HG, PVT1, RMRP, SNHG15, and SOCS2-AS1. Changes differing between strains were measured for APTR, FIRRE, HOTAIR, HOXD-AS1, KCNQ1OT1, LINC00968, LINC01105, lnc-SGK1, MEG3, MHRT, MIAT, MIR17HG, MIR155HG, NEAT1, NeST, NRON, and PACER. Our findings suggest roles for lncRNAs in regulating retinal Müller cell immune responses to *T. gondii*, and encourage future studies on lncRNA as biomarkers and/or drug targets in ocular toxoplasmosis.

Keywords: *Toxoplasma gondii*; toxoplasmosis; human; eye; retina; Müller cells; long non-coding RNA

1. Introduction

Toxoplasma gondii is a ubiquitously distributed protozoan parasite that may infect any warm blooded animal [1]. Clinical disease in humans is related to localization to the central nervous system. Ocular toxoplasmosis follows the entry of *T. gondii* into and replication within the retina, which is associated with a vigorous inflammatory reaction; the inflammation may reach other ocular tissues, such as choroid, vitreous, or more rarely the optic nerve [1,2]. Ultimately the reaction resolves, but leaves scars in the retina that are associated with the parasite encystment. Subsequent rupture of a retinal cyst leads to the reactivation of the condition, followed by a new attack of inflammation. Although ocular toxoplasmosis is a worldwide disease, differences in clinical manifestations are observed, and are related to the host genetics, geographical region, and parasite genotype [3–5]. In Western Europe and North America, where 2% of the *T. gondii* seropositive population have retinal lesions, most of the parasite strains belong to type I, II, and III, and haplogroup 12 clonal lineages [6,7]. On the contrary, in South America, many non-clonal haplogroups are found [8–10], which are linked to more severe presentations and a higher prevalence of retinal lesions, reaching as high as 17% [11–13].

Müller cells are a unique retinal cell population with multiple biological functions [14]. They are the predominant glial cell of the eye, extending between the internal and external limiting membranes of the retina and providing support for all neurons. Müller cells are a first line of defense during retinal infection, and are involved in the innate immune response to a pathogen by producing cytokines and chemokines necessary to attract and activate leukocytes [15–17]. However, they are unable to control tachyzoite proliferation alone [18]. Müller cells also are a preferential target of *T. gondii* in the human retina—Furtado et al. [19] highlighted that Müller cells are more susceptible to the infection than retinal neurons. Along with ganglion neuronal cells, Müller cells are the intraocular cell population that harbors the latent form of the parasite—the bradyzoite [20–23].

Gene expression in both healthy and pathological microenvironments is directed in part by a diverse group of regulatory long non-coding RNAs (lncRNAs) [24]. Long non-coding RNAs are defined by lack of protein-coding ability and a length greater than 200 nucleotides. However, recent studies have demonstrated that some lncRNAs encode micropeptides with possible biological activity [25,26]. Most lncRNAs are transcribed by RNA polymerase II, and may be spliced, polyadenylated, and 5' capped. Conservation across species is generally poor, and lncRNAs usually have low abundance in cells, with a few exceptions, such as metastasis associated lung adenocarcinoma transcript 1 (MALAT1), nuclear paraspeckle assembly transcript 1 (NEAT1), and homeobox gene transcript antisense RNA (HOTAIR) [27]. Expression is cell and/or tissue-specific, and may vary over time and in response to local molecular conditions. According to cellular localization, and secondary and tertiary structures, lncRNAs may bind DNA, RNA, and protein to influence molecular functions in *cis* or *trans* [28,29]. As regulators of gene expression, lncRNAs participate in a wide range of biological processes [30,31], acting in multiple overlapping molecular roles, including as signalers, enhancers, scaffolds, decoys, and guides [32]. Dysregulation of lncRNAs has been connected to a variety of pathologies, such as cancers, immune and infectious diseases, neurological conditions, and genetic disorders [30,33].

During infection, host lncRNA expression in myeloid and non-myeloid cells may change, consistent with a role in the regulation of host–pathogen interactions and the outcome of infection [28]. Certain lncRNAs promote pathogen clearance (e.g., host nettoie salmonella pas Theiler's (NeST) in *Salmonella enterica* infection) [34], whereas others facilitate survival of the pathogen (e.g., host non-coding repressor of nuclear factor of activated T-cells (NRON) during human immunodeficiency virus infection) [35]. The involvement of lncRNAs in *T. gondii* infection of Müller cells is unstudied. Indeed, there is little published literature on the role of Müller cells during a *T. gondii* infection [18,19,36], or during intracellular pathogen infection in general [37,38]. Here, we were interested in the lncRNA response of Müller cells to infection with virulent strains of *T. gondii*, with a focus on the acute immune response. We first examined expression of 35 human lncRNAs with known immunologic activities in primary retinal Müller cells and the MIO-M1 cell line. Then, we used reverse transcription real-time quantitative polymerase chain reaction (RT-qPCR) to follow expressed lncRNAs over time in MIO-M1 cells infected with two natural virulent strains of *T. gondii*—GT1 (type I, haplogroup 1, common in the United States and Western Europe) and GPHT (haplogroup 6, common in South America).

2. Results

2.1. Expression of Long Non-Coding RNA in Human Retinal Müller Cells

We selected 35 lncRNAs for investigation—these lncRNAs were identified on the basis of a literature search directed at human lncRNA with role(s) in the immune responses. Prior to investigating the potential involvement of retinal Müller cell lncRNAs in the immune response to *T. gondii*, we first assessed expression of these 35 lncRNAs by cells under baseline conditions. We studied primary Müller cells, isolated from three cadaveric human donors, and the MIO-M1 human Müller cell line. Because of the large number of cells needed for the infectivity studies, it was necessary to use a cell line, and, thus, this first stage of our work served to confirm that the lncRNAs to be studied in the MIO-M1 cell line were also expressed by primary Müller cells.

Twenty-eight of the 35 selected lncRNAs were expressed in both primary Müller cells and the MIO-M1 Müller cell line (Figure 1): alu-mediated P21 transcriptional regulator (APTR), B-Raf proto-oncogene, serine/threonine kinase-activated non-protein coding RNA (BANCR), cytoskeleton regulator RNA (CYTOR or LINC00152), functional intergenic repeating RNA element (FIRRE), forkhead box D3-antisense RNA 1 (FOXD3-AS1), growth arrest specific 5 (GAS5), glutathione S-transferase theta 1 antisense RNA 1 (GSTT1-AS1 or lncRNA-CD244), HOTAIR, homeobox D cluster antisense RNA 1 (HOXD-AS1), potassium voltage-gated channel subfamily Q member 1 opposite strand/antisense transcript 1 (KCNQ1OT1), long intergenic non-protein coding RNA 968 (LINC00968), long non-coding RNA serum and glucocorticoid-inducible kinase (lnc-SGK1), lung cancer associated transcript 1 (LUCAT1), MALAT1, maternally expressed 3 (MEG3), myosin heavy chain associated RNA transcripts (MHRT), myocardial infarction associated transcript (MIAT or GOMAFU), MIR17 host gene (MIR17HG), MIR22 host gene (MIR22HG), MIR143 host gene (MIR143HG or CARMN), MIR155 host gene (MIR155HG), NEAT1, NRON, P53 upregulated regulator of P53 levels (PURPL), plasmacytoma variant translocation 1 (PVT1), RNA component of mitochondrial RNA processing endoribonuclease (RMRP), small nucleolar RNA host gene 15 (SNHG15), and suppressor of cytokine signaling 2-antisense RNA 1 (SOCS2-AS1).

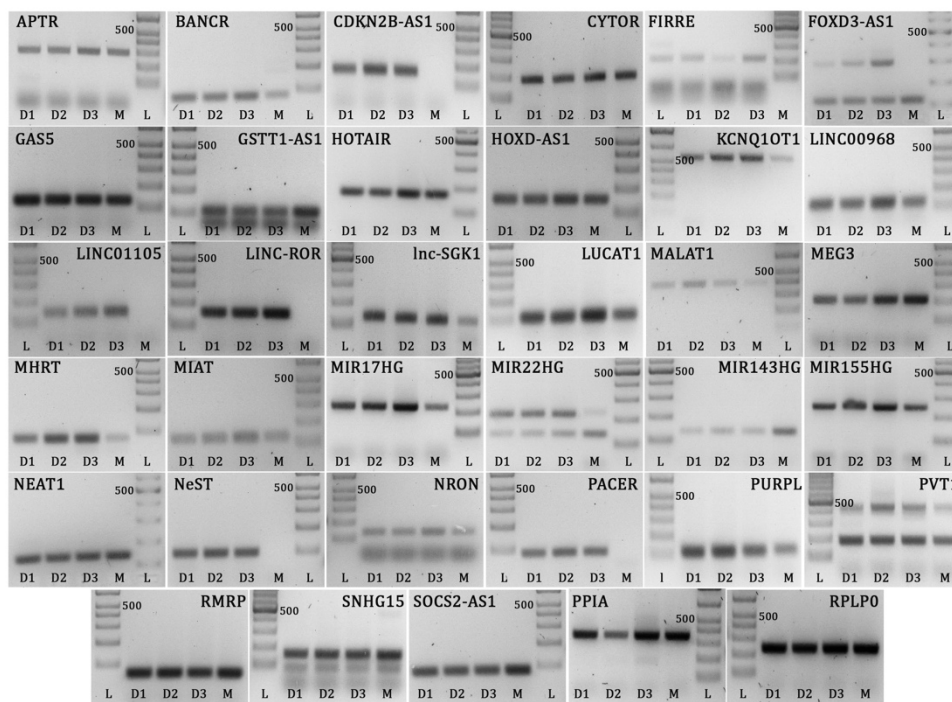


Figure 1. Gel images showing Müller cell long non-coding RNAs and reference gene amplicons run on 2% or 3% agarose gel. L = DNA ladder, D1 = human donor cell isolate 1, D2 = human donor cell isolate 2, D3 = human donor cell isolate 3, M = MIO-M1 cell line. Expected product sizes: APTR = 300 bp, BANCR = 80 bp, CDKN2B-AS1 = 169 bp, CYTOR = 187 bp, FIRRE = 215 bp, FOXD3-AS1 = 118 bp, GAS5 = 127 bp, GSTT1-AS1 = 105 bp, HOTAIR = 168 bp, HOXD-AS1 = 149 bp, KCNQ1OT1 = 567 bp, LINC00968 = 126 bp, LINC01105 = 137 bp, LINC-ROR = 151 bp, lnc-SGK1 = 131 bp, LUCAT1 = 114 bp, MALAT1 = 396 bp, MEG3 = 187 bp, MHRT = 73 bp, MIAT = 122 bp, MIR17HG = 221 bp, MIR22HG = 136/219 bp, MIR143HG = 128 bp, MIR155HG = 247 bp, NEAT1 = 137 bp, NeST = 94 bp, NRON = 133 bp, PACER = 90 bp, PURPL = 120 bp, PVT1 = 179 bp, RMRP = 67 bp, SNHG15 = 155 bp, SOCS2-AS1 = 83 bp, PPIA = 355 bp, RPLP0 = 235 bp. Multiple bands on same gel (FOXD3-AS1, GSTT1-AS1, MIR22HG, PVT1, and SNHG15) represent transcript variants, which were confirmed by sequencing. Bands at lower edge of gels represent primer dimer products. Controls prepared with no template did not amplify.

Five of the 35 selected lncRNAs that were detected in primary Müller cells were not expressed in the MIO-M1 Müller cell line under non-stimulated conditions (Figure 1): long intergenic non-protein coding RNA, regulator of reprogramming (LINC-ROR), LINC01105, nettoie salmonella pas Theiler's (NeST), cyclin-dependent kinase inhibitor 2B-antisense RNA 1 (CDKN2B-AS1), and PTGS2 antisense NFKB1 complex-mediated expression regulator RNA (PACER). The larger of the two FOXD3-AS1 transcripts was also not detected in MIO-M1 cells. Two of the 35 selected lncRNAs—LINC00305 and negative regulator of interferon response (NRIR or lncRNA-CMPK2)—were not expressed in primary cells or the cell line (data not shown), and therefore were not evaluated further in this work.

2.2. Time Course of *T. gondii* Growth in Human Retinal Müller Cells

Growth of GT1 and GPHT strain *T. gondii* tachyzoites in the MIO-M1 human retinal Müller cell line was assessed over 36 h by RT-qPCR for *T. gondii* surface antigen 1 (SAG1) (Figure 2). The level of SAG1 transcript was stable at low levels at 4 and 12 h post infection, consistent with invasion by the parasite. A marked increase in SAG1 expression was observed for cells infected with both strains at 24 h, indicating rapid intracellular replication of the parasite. By 36 h post-infection, there was no further increase in SAG1 expression, consistent with tachyzoite preparing to egress the cells, which typically occurs by approximately 48 h.

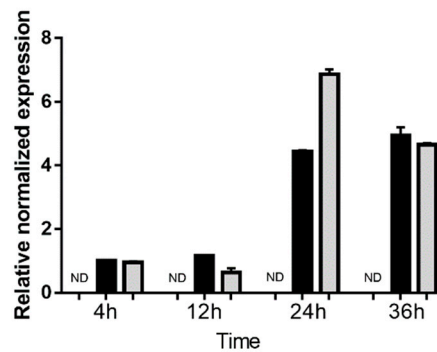


Figure 2. Expression of surface antigen 1 (SAG1) in human retinal Müller cells infected with *T. gondii* tachyzoites. Graph shows normalized SAG1 transcript expression in uninfected versus GT-1 and GPHT strain-infected MIO-M1 cells (multiplicity of infection = 5; evaluated time points post-infection = 4, 12, 24, and 36 h). Reference genes were ribosomal protein lateral stalk subunit P0 (RPLP0) and peptidylprolyl isomerase A (PPIA). $n = 3$ cultures/condition. Bars represent mean normalized expression, and error bars indicate standard deviation. Black columns represent GT1 strain-infected, and grey columns represent GPHT strain-infected.

2.3. Expression of Long Non-Coding RNAs in Human Retinal Müller Cells during *T. gondii* Infection

The expression kinetics of 33 immune-related lncRNAs in Müller cells during *T. gondii* infection was evaluated by RT-qPCR in the MIO-M1 human retinal Müller cell line following infection with GT1 or GPHT strain tachyzoites. PURPL and CDKN2B-AS1 were not detected in these experiments (data not shown). For the remaining 31 lncRNAs, two patterns of expression were observed: (1) similarity in the changes in, or stability of, gene expression in infected versus uninfected Müller cells, when comparing infections by GT1 or GPHT strain tachyzoites (Figure 3), and (2) differences in the changes in, or stability of, gene expression in infected versus uninfected Müller cells, when comparing infections by GT1 or GPHT strain tachyzoites (Figure 4).

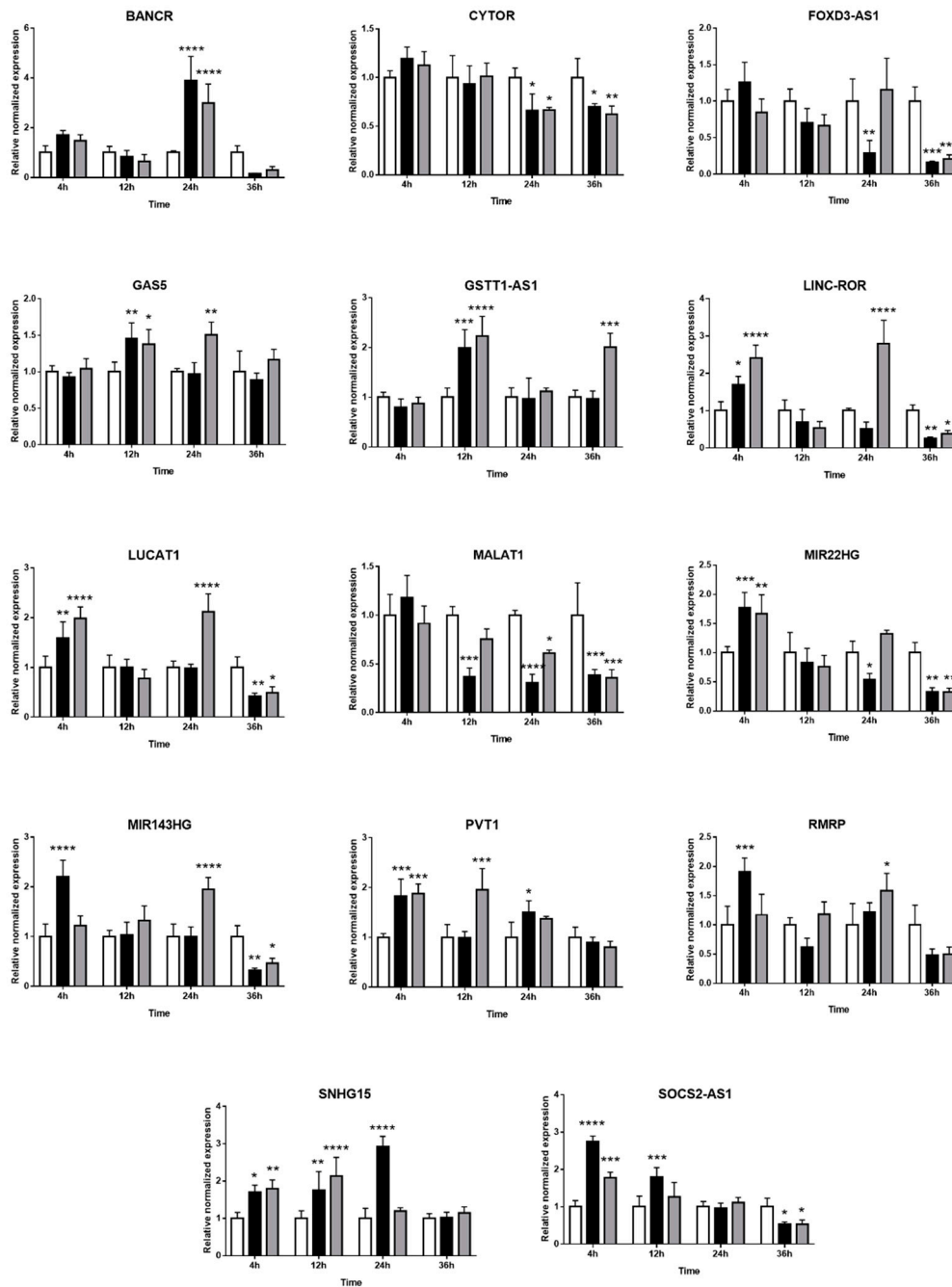


Figure 3. Expression of long non-coding RNAs in human retinal Müller cells infected with *T. gondii* tachyzoites with similarity in response to parasite strains. Graphs show normalized lncRNA expression in uninfected versus GT-1 and GPHT strain-infected MIO-M1 cells (multiplicity of infection = 5; evaluated time points post-infection = 4, 12, 24, and 36 h). Reference genes were ribosomal protein lateral stalk subunit P0 (RPLP0) and peptidylprolyl isomerase A (PPIA). Data were analyzed by two-way ANOVA with Bonferroni post-test. $n = 3$ cultures/condition. Bars represent mean normalized expression, and error bars indicate standard deviation. White columns represent uninfected, black columns represent GT1 strain-infected, and grey columns represent GPHT strain-infected. * $p < 0.05$, ** $p < 0.01$, *** $p < 0.001$, and **** $p < 0.0001$.

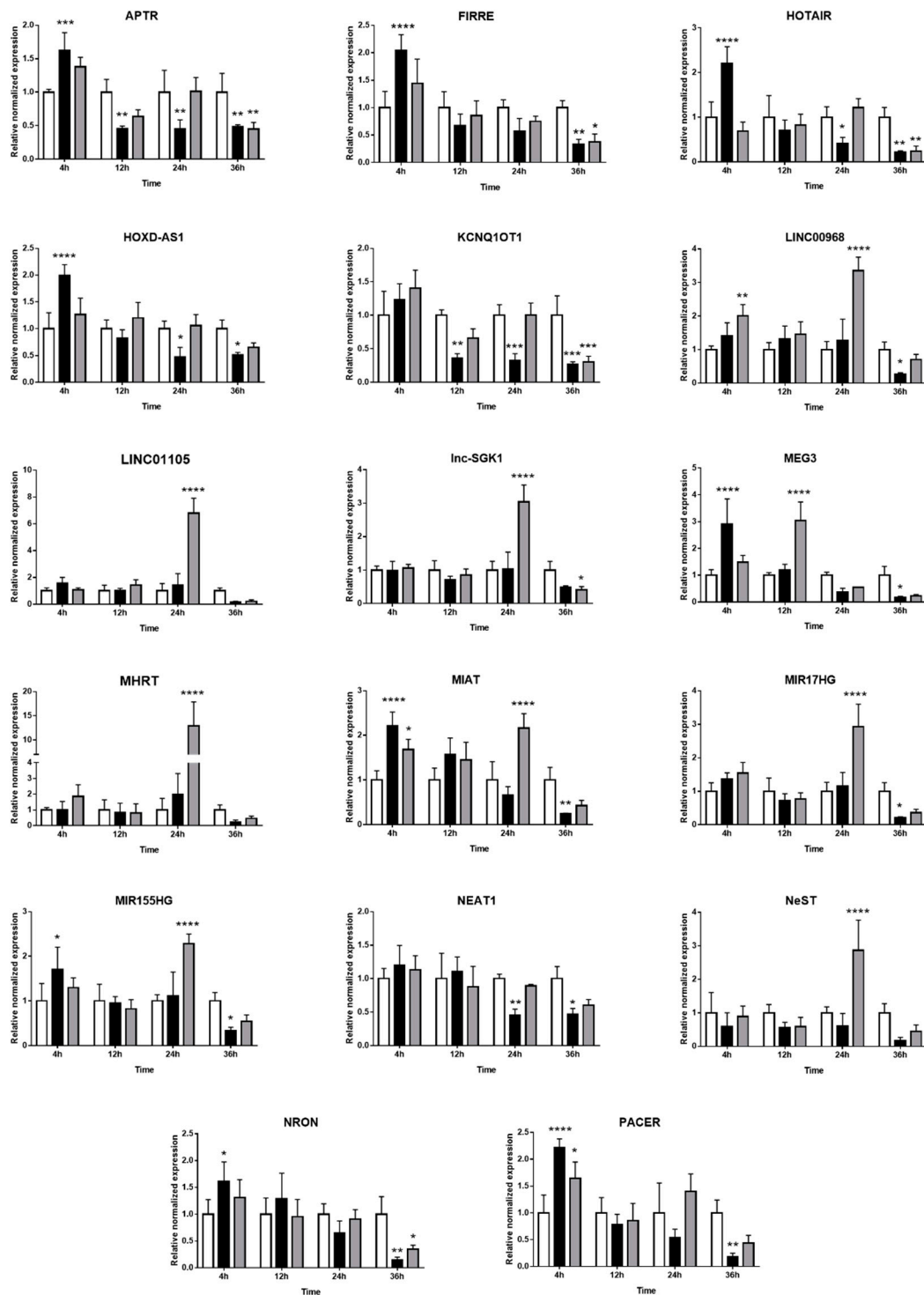


Figure 4. Expression of long non-coding RNAs in human retinal Müller cells infected with *T. gondii* tachyzoites with differences in response to parasite strains. Graphs show normalized lncRNA expression in uninfected versus GT-1 and GPHT strain-infected MIO-M1 cells (multiplicity of infection = 5; evaluated time points post-infection = 4, 12, 24, and 36 h). Reference genes were ribosomal protein lateral stalk subunit P0 (RPLP0) and peptidylprolyl isomerase A (PPIA). Data were analyzed by two-way ANOVA with Bonferroni post-test. $n = 3$ cultures/condition. Bars represent mean normalized expression, and error bars indicate standard deviation. White columns represent uninfected, black columns represent GT1 strain-infected, and grey columns represent GPHT strain-infected. * $p < 0.05$, ** $p < 0.01$, *** $p < 0.001$, and **** $p < 0.0001$.

Among the common changes in lncRNAs that occurred in human retinal Müller cells infected with either *T. gondii* strain, as presented in Figure 3, some lncRNAs (i.e., LINC-ROR, LUCAT1, MIR22HG, MIR143HG, and SOCS2-AS1) were upregulated in the first 24 h post-infection as tachyzoites actively replicated, and downregulated at 36 h post-infection as tachyzoites prepared to egress. Other lncRNAs (i.e., BANCR, GAS5, GSTT1-AS1, PVT1, RMRP, and SNHG15) increased at one or more time-points during infection; BANCR was highly increased in infected cells, but only at 24 h. In contrast, CYTOR, FOXD3-AS1, and MALAT1 were consistently downregulated during the infection.

As presented in Figure 4, the two *T. gondii* strains influenced the expression of some lncRNAs in human retinal Müller cells in different ways. More lncRNAs were modulated during infection with GPHT—primarily manifested as high upregulation at 24 h—while infection with GT1 regulated the expression of lncRNAs in a more sustained manner. Thus, expression of LINC00968, LINC01105, lnc-SGK1, MHRT, MIR17HG, and NeST were only or largely impacted in GPHT infection. Some lncRNAs were differentially modulated depending on the parasite strain. APTR, FIRRE, HOTAIR, HOXD-AS1, MEG3, MIAT, MIR155HG, NRON, and PACER were upregulated at 4 h post-infection, and then immediately downregulated in GT1 infection, whereas they were only downregulated in GPHT infection at 36 h post-infection or not at all. LINC00968 was upregulated during the first 24 h of GPHT infection, but it was downregulated at 36 h after GT1 infection. NEAT1 and HOXD-AS1 expression were only modulated by the GT1 strain, whereas GPHT alone influenced LINC01105, lnc-SGK1, MHRT, and NeST expression.

At 36 h post-infection, consistent with imminent tachyzoite egress and Müller cell death, the majority of lncRNAs were downregulated in infected cells, with the exception of GSTT1-AS1, which was increased in GPHT-infected cells. Some lncRNAs were not significantly regulated in this final stage of the infection—in cells infected with both strains, BANCR, GAS5, LINC01105, MHRT, NeST, PVT1, RMRP, and SNHG15; in cells infected with GT1, GSTT1-AS1, and lnc-SGK1; and in cells infected with GPHT, LINC00968, MIAT, MIR17HG, HOXD-AS1, MIR155HG, NEAT1, and PACER.

3. Discussion

Little research has been published on the response of human retinal Müller cells to infection with *T. gondii*, although these cells are the key supporting cells within the retina, and ocular toxoplasmosis is a common retinal infection. We investigated the expression of lncRNAs in Müller cells infected with *T. gondii* tachyzoites to explore potential involvement of these regulatory molecules in ocular toxoplasmosis, focusing primarily on lncRNAs involved in the immune response and inflammation. We studied two virulent parasite strains for clear relevance to human disease—GT1 and GPHT. We measured significant changes at one or more time-points post-infection in the large majority of the lncRNAs that we studied (i.e., 31 of 35 lncRNAs). Although similarities in lncRNA expression were observed in both strains, more than half the lncRNAs studied were found to be differentially responsive to the strain. Interestingly, a few lncRNAs were modulated by one strain only—HOXD-AS1 and NEAT1 in GT1 infection, and LINC01105, lnc-SGK1, MHRT, and NeST in GPHT infection.

Long non-coding RNAs are involved in many aspects of the immune response, including immune homeostasis and inflammation, and the processes of leukocyte development, proliferation, and activation [39]. It is also clear that infectious pathogens may influence the expression of host lncRNA [28]. Using a microarray-based profiling approach, Liu et al. [37] and Menard et al. [38] independently evaluated the global lncRNA transcriptome in cells infected with *T. gondii* tachyzoites. There are many methodological differences between our investigation and these two studies, including molecular biological methods, strains of parasite, and host species and host cell population, all of which may impact experimental results. However, taking a discovery approach, both other groups found that the infection dysregulated substantial numbers of lncRNAs involved in the immune response. Liu et al. [37] used an array that covered 40,173 human lncRNAs to study infection of human neonatal fibroblasts by the type II avirulent strain ME49 strain—4525 lncRNAs were up-regulated, and 1519 lncRNAs were down-regulated, and coding-non-coding co-expression network analyses showed

lncRNAs were involved in the expression of multiple immune-related proteins. Menard et al. [38] examined differential expression of lncRNAs in mouse bone marrow-derived macrophages infected with the type I virulent RH strain or the type II avirulent PTG strain—893 lncRNAs were up-regulated, and 875 lncRNAs were down-regulated, and gene ontology analyses demonstrated that these lncRNAs participated in many immune-related biological processes [38]. This second study highlighted a difference in the cellular response to the virulent and avirulent *T. gondii* strains, which was explained in part by a direct effect of the parasite ROP16 protein on host cell lncRNA expression [38].

In our results—obtained in human retinal Müller cells, which have direct relevance to ocular toxoplasmosis—LINC01105, BANCR, MIR17HG, MIR155HG, lnc-SGK1, MEG3, KCNQ1OT1, NEAT1, NeST, and MALAT1 were the most dysregulated lncRNAs with known immunologic activities. NeST is of particular interest, as it may act to boost a Th1 response by inducing IFN- γ transcription [34], and IFN- γ is critical to control the growth of *T. gondii* [40]. However, IFN- γ is produced primarily by activated lymphocytes [41], and a transcriptomic profiling study in progress indicates that human retinal Müller cells do not express this cytokine (data not shown). This lncRNA is transcribed anti-sense from a region of the genome that encodes interleukin (IL)-22 and IL-26, members of the IL-10 cytokine family, which may have anti-microbial activities [42]. The GPHT strain triggers earlier and higher expression of NeST than the GT1 strains, and this strain differential in the Müller cell immune response might have implications for clinical manifestations.

Other Müller cell lncRNAs that show significant changes in response to *T. gondii* infection—MEG3, MIR17HG and lnc-SGK1—are involved in regulation of the Th17 immune response [43–46]. This adaptive immune response, and production of IL-17 and IL-23 in particular, has been strongly implicated in the pathogenesis of ocular toxoplasmosis [47,48]. MEG3 is defined as a tumor suppressor, but also regulates the balance of Treg cells and Th17 cells; downregulation of MEG3 increases forkhead box P3 (FOXP3) expression and inhibits retinoic acid receptor-related orphan receptor γ t (ROR γ t) expression, to tip the balance in favor of Treg cells [45,46]. On the other hand, MIR17HG and lnc-SGK1 promote the Th17 response [43,44]. Thus, our results suggest increased MEG3 may counterbalance the effects of increased MIR17HG and lnc-SGK1 in *T. gondii* infection. We also observed strong upregulation of BANCR in Müller cells at 24 h after infection with the virulent strains of *T. gondii* that we studied. An induction of BANCR by IL-13 has been demonstrated in vitro using a human esophageal epithelial cell line, ultimately leading to pro-inflammatory gene expression [49]. These molecular observations are in keeping with results of intraocular cytokinome profiling in South American patients, which identify IL-13 as a biomarker for severe ocular toxoplasmosis [5].

We also observed changes in several lncRNAs that have been implicated in cellular proliferation, invasion, and migration. LINC00968 has been studied mainly in cancer pathogenesis; it may promote tumor cell growth, migration, and invasion upon activation of Wnt/ β -catenin or by targeting cyclin-A2 [50,51]. LINC00968 also may lead to apoptosis of the cell by recruiting enhancer of zeste homolog 2 (EZH2) to the promoter of p21, which inhibits p21 expression [52]. A critical role of BANCR in progression and metastasis of malignant melanoma and bronchial carcinoma is linked to the MAPK pathway [53,54]. On the other hand, LINC-ROR, first described as regulator of reprogramming [55], promotes c-Myc expression and interacts with p53 to generate an autoregulatory feedback loop that influences cell cycle progression and apoptosis [56]. *T. gondii* may have pro- or anti-proliferative effects, depending on the host cell population [57–61].

For this work on *T. gondii* infection, we employed the MIO-M1 human retinal Müller cell line in place of primary Müller cells. This was necessary, as we needed relatively large numbers of cells than could be generated reliably from individual paired human retinæ. Freshly isolated human Müller cells are extremely slow growing. MIO-M1 cell line was spontaneously immortalized in 2002 from the eyes of a 68 year old female corneal donor [62], and is well characterized and widely used to study mechanisms of retinal disease. The MIO-M1 cell line provides reasonable transcriptomic fidelity to primary human Müller cells. As recently reported (bioRxiv unpublished preprint: <https://doi.org/10.1101/425223>), S.W. Lukowski et al. profiled the MIO-M1 cell line against other retinal cell types, and identified

a glial cell transcriptome, with similarity to that of astrocytes, as well as Müller cells. Apart from CDKN2B-AS1, all the lncRNAs that we identified in primary Müller cells were also expressed by MIO-M1 cells, either at baseline or as a result of infection. However, alterations in the expression of a specific lncRNA of interest could be confirmed in primary Müller cells for the time-point at which we measured maximum dysregulation.

In conclusion, our work opens up a new area of research on the involvement of lncRNAs in the interaction between *T. gondii* and human retinal host cells, with implications for the pathogenesis—and ultimately the management—of ocular toxoplasmosis. Despite the fact that understanding of lncRNA activity in infectious diseases is still relatively limited, their major involvement as regulators of gene expression make lncRNAs attractive as therapeutic targets or biomarkers. Our work is limited to a descriptive *in vitro* study, without mechanistic experiments designed to test the roles of lncRNA in *T. gondii* infection in retinal cells *in vitro* or in ocular toxoplasmosis *in vivo*. We observed changes over the course of *T. gondii* infection of retinal Müller cells for almost all the lncRNAs that we studied. These changes were often impacted by parasite strain, and future work might be directed at evaluating other strains that may cause ocular toxoplasmosis, including avirulent strains. In addition, evaluation of lncRNA expression in other human retinal cells that participate in the immune response to *T. gondii*, such as microglia and pigment epithelial cells, could be extremely informative.

4. Materials and Methods

4.1. Human Subjects

The use of human eyecups for this research was approved by the Southern Adelaide Clinical Human Research Ethics Committee (protocol number: 175.13). Three human cadaver donor eyecup pairs were obtained from the Eye Bank of South Australia (Adelaide, Australia). The three donors were aged 62 to 71 years at death, and the time from death to processing of the eyecups averaged 11 h.

4.2. Cell Culture

The MIO-M1 (Moorfields Eye Hospital/University College London Institute of Ophthalmology—Müller 1) cell line (kind gift of G. Astrid Limb, PhD, and Peng T. Khaw, MD, PhD, University College London, London, UK) [62] was cultured in Dulbecco's modified Eagle's medium (DMEM; Thermo Fisher Scientific-GIBCO, Grand Island, NY, USA) with 10% heat-inactivated fetal bovine serum (FBS; Bovogen Biologicals, Keilor East, Australia or Thermo Fisher Scientific-GIBCO) at 37 °C and 5% CO₂ in air.

Retinae from donor eyecup pairs were individually digested in 0.5 mg/mL of Dispase II in phosphate-buffered saline (PBS) with 2% FBS for 10 min at 37 °C. Digested tissue was dissociated by pipetting, passed through a 30 µm strainer, and pelleted by centrifugation. Cells were resuspended in DMEM, Non-Essential Amino Acids Solution, GlutaMAX Supplement, 1 mM sodium pyruvate, 100 U/mL penicillin–100 µg/mL streptomycin (all from Thermo Fisher Scientific-GIBCO), and 10% FBS, plated into 10 cm diameter dishes, and incubated at 37 °C and 5% CO₂ in air. Half the medium was changed after 5 days in culture and then once per week.

The phenotype of retinal cells isolated by this method was assessed on expression of Müller markers: cellular retinaldehyde binding protein (CRALBP), glutamine synthetase (GS), vimentin, and glial fibrillary acidic protein (GFAP), as presented in Figure 5. Cells were fixed with 4% paraformaldehyde for 10 min, permeabilized with 0.2% Triton X-100 for 5 min, and blocked for 1 h with 2% bovine serum albumin (BSA) and 0.05% Triton X-100 in PBS at room temperature. Cells were incubated overnight at 4 °C with primary antibody diluted to working concentration in 2% BSA–0.05% Triton X-100 in PBS (Supplementary Table S1), subsequently with Alexa 488- or 594-conjugated secondary antibody for 1 h at room temperature, and finally with 4',6-diamidino-2-phenylindole stain for 2 min. Between steps, cells were washed three times with 0.1% Tween in PBS for 5 min. Immunolabelled cells were imaged on the IX53 Inverted Microscope (Olympus, Tokyo, Japan).

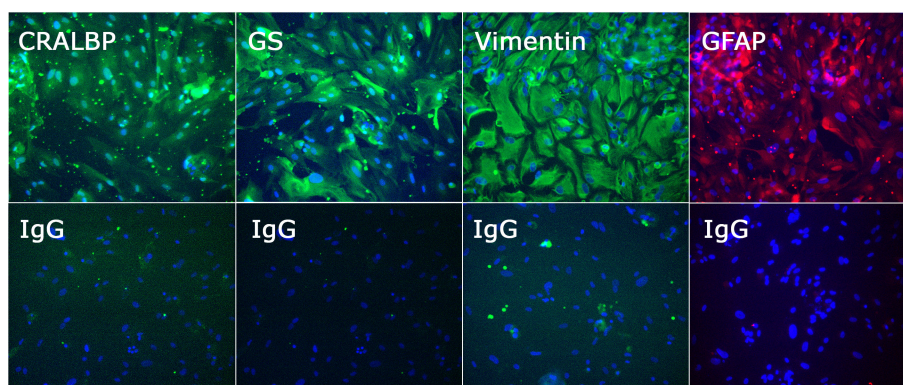


Figure 5. Photomicrographs of Müller cells isolated from human retinæ and phenotyped by immunocytochemistry for cellular retinaldehyde binding protein (CRALBP), glutamine synthetase (GS), vimentin, and glial fibrillary acidic protein (GFAP), with negative control labelled with species-matched primary antibody (IgG). Cells stained positively for CRALBP, GS, vimentin, and GFAP; staining artefacts were visible in the negative control, but the labelling pattern was clearly different. Alexa Fluor 488 (green) or Alexa Fluor 594 (red) with DAPI nuclear counterstain (blue). Original magnification: 200×.

4.3. Parasite Culture

Natural isolate *T. gondii* strains were maintained in tachyzoite form by serial passage in confluent human dermal fibroblast monolayers (Cascade Biologics, Portland, OR, USA) in DMEM supplemented with 1% heat-inactivated FBS at 37 °C and 5% CO₂ in air—GT1 (type I, haplogroup 1) and GPHT (haplogroup 6) (kind gifts of Dr. Jitender P. Dubey, U.S. Department of Agriculture, Beltsville, MD, and Dr. L. David Sibley, Washington University, St Louis, MO, USA) [63,64]. Parasite viability was evaluated by plaque assay in fibroblast monolayers, and required to be at least 15%, which is the expected viability of freshly egressed tachyzoites [65].

4.4. Infection of MIO-M1 Cells

Confluent monolayers of MIO-M1 cells in 6-well plates were infected with freshly egressed GT1 or GPHT *T. gondii* tachyzoites in DMEM with 1% heat-inactivated FCS at a multiplicity of infection of 5, or treated with fresh medium alone ($n = 3$ wells per condition). Cell monolayers were incubated at 37 °C and 5% CO₂ in air, and harvested at 4, 12, 24, and 36 h post-infection.

4.5. RNA Isolation and Reverse Transcription

Total RNA was extracted from primary retinal Müller cells and MIO-M1 cells with TRIzol Reagent (Thermo Fisher Scientific-Ambion, Carlsbad, CA, USA), used according to the retailer's instructions, and frozen at −80 °C. RNA concentration was determined by spectrophotometry on the NanoDrop 2000 (Thermo Fisher Scientific, Wilmington, DE, USA). Reverse transcription was performed using the iScript Reverse Transcription Supermix for RT-qPCR (Bio-Rad, Hercules, CA, USA), with 100 ng (PCR) or 500 ng (qPCR) of RNA template yielding 20 µL cDNA.

4.6. Polymerase Chain Reaction

PCR was performed on the T100 Thermocycler (Bio-Rad) using 1.5 µL of cDNA diluted to 1:5, 2.5 µL of 10× PCR buffer (Bio-Rad), 0.5 µL of 10 mM dNTP mix, 1.2 µL of 25 mM magnesium chloride, 1.25 µL each of 20 µM forward and reverse primers (Supplementary Table S2), 0.2 µL of HotStar Taq Polymerase, and 16.6 µL of nuclease-free water for each reaction. Amplification consisted of a pre-cycling hold at 95 °C for 5 min, 40 cycles of denaturation for 30 s at 95 °C, annealing for 30 s at 60 °C (or 58.2 °C for SNHG15, or 63.3 °C for MIR143HG), extension for 1 min at 72 °C, and a post-extension hold at 72 °C for 5 min. Sizes of PCR products were confirmed by electrophoresis with SYBR Safe

DNA Gel Stain (Thermo Fisher Scientific-Invitrogen, Carlsbad, CA, USA) on 2% or 3% agarose gel, depending on the expected product size.

4.7. Quantitative Real-Time Polymerase Chain Reaction

The RT-qPCR was performed on the CFX Connect Real-Time PCR Detection System (Bio-Rad) using 2 µL of cDNA diluted to 1:10, 4 µL of iQ SYBR Green Supermix (Bio-Rad), 1.5 µL each of 20 µM forward and reverse primers (Supplementary Table S2), and 11 µL of nuclease-free water for each reaction. Amplification consisted of a pre-cycling hold at 95 °C for 5 min, 40 cycles of denaturation for 30 s at 95 °C, annealing for 30 s at 60 °C, extension for 30 s at 72 °C, and a post-extension hold at 75 °C for 1 s. A melting curve, representing a 1 s hold at every 0.5 °C between 70 °C and 95 °C, was generated to confirm that a single peak was produced for each primer set. The cycle threshold was measured, with Cq determination mode set to regression. Relative expression was determined using the Pfaffl mathematical model [66], and normalized to two stable reference genes: ribosomal protein lateral stalk subunit P0 (RPLP0) and peptidylprolyl isomerase A (PPIA). Stability of reference gene expression was assessed using the method described by Hellemans et al. [67], which we have used in previous work [68]; this involves calculation of the gene-stability measure (M-value) and the coefficient of variance (CV-value), and requires an M-value of less than 0.5 and a CV-value of less than 0.25. These calculations were performed with the Gene Expression Analysis module of CFX Manager v3.1 software (Bio-Rad). Transcript expression in *T. gondii*-infected and uninfected MIO-M1 cells were compared by two-way ANOVA with Bonferroni post-test. A *p*-value less than 0.05 was taken to indicate statistical significance.

Supplementary Materials: The following are available online at <http://www.mdpi.com/2311-553X/5/4/48/s1>, Table S1: Primary antibodies for retinal Müller cell markers; Table S2: Primer sequences and product sizes for gene transcripts.

Author Contributions: Conceptualization, E.R., B.A. and J.S.; methodology, E.R., B.A., Y.M., L.A. and J.S.; formal analysis, E.R. and J.S.; investigation, E.R., Y.M. and L.A.; data curation, E.R. and Y.M.; writing—original draft preparation, E.R. and J.S.; writing—review and editing, E.R., B.A., Y.M., L.A. and J.S.; supervision, B.A. and J.S.; project administration, J.S.; funding acquisition, E.R. and J.S.

Funding: This work was supported in part by grants from Australian Research Council (FT130101648, Dr. Smith) and Fondation de France (00069556, Dr. Rochet).

Acknowledgments: The authors wish to thank Ms. Janet Matthews for her administrative work in the preparation of the manuscript.

Conflicts of Interest: The authors declare no conflict of interest. The funders had no role in the design of the study; in the collection, analyses, or interpretation of data; in the writing of the manuscript, or in the decision to publish the results.

References

1. Furtado, J.M.; Winthrop, K.L.; Butler, N.J.; Smith, J.R. Ocular toxoplasmosis I: Parasitology, epidemiology and public health. *Clin. Exp. Ophthalmol.* **2013**, *41*, 82–94. [[CrossRef](#)] [[PubMed](#)]
2. Butler, N.J.; Furtado, J.M.; Winthrop, K.L.; Smith, J.R. Ocular toxoplasmosis II: Clinical features, pathology and management. *Clin. Exp. Ophthalmol.* **2013**, *41*, 95–108. [[CrossRef](#)] [[PubMed](#)]
3. Albuquerque, M.C.; Aleixo, A.L.; Benchimol, E.I.; Leandro, A.C.; das Neves, L.B.; Vicente, R.T.; Bonecini-Almeida Mda, G.; Amendoeira, M.R. The IFN-gamma +874T/A gene polymorphism is associated with retinochoroiditis toxoplasmosis susceptibility. *Mem. Inst. Oswaldo Cruz* **2009**, *104*, 451–455. [[CrossRef](#)] [[PubMed](#)]
4. Cordeiro, C.A.; Moreira, P.R.; Bessa, T.F.; Costa, G.C.; Dutra, W.O.; Campos, W.R.; Orefice, F.; Young, L.H.; Teixeira, A.L. Interleukin-6 gene polymorphism (−174 G/C) is associated with toxoplasmic retinochoroiditis. *Acta Ophthalmol.* **2013**, *91*, e311–e314. [[CrossRef](#)] [[PubMed](#)]

5. De-la-Torre, A.; Sauer, A.; Pfaff, A.W.; Bourcier, T.; Brunet, J.; Speeg-Schatz, C.; Ballonzoli, L.; Villard, O.; Ajzenberg, D.; Sundar, N.; et al. Severe South American ocular toxoplasmosis is associated with decreased Ifn-gamma/Il-17a and increased Il-6/Il-13 intraocular levels. *PLoS Negl. Trop. Dis.* **2013**, *7*, e2541. [[CrossRef](#)] [[PubMed](#)]
6. Howe, D.K.; Sibley, L.D. *Toxoplasma gondii* comprises three clonal lineages: Correlation of parasite genotype with human disease. *J. Infect. Dis.* **1995**, *172*, 1561–1566. [[CrossRef](#)] [[PubMed](#)]
7. Khan, A.; Dubey, J.P.; Su, C.; Ajioka, J.W.; Rosenthal, B.M.; Sibley, L.D. Genetic analyses of atypical *Toxoplasma gondii* strains reveal a fourth clonal lineage in North America. *Int. J. Parasitol.* **2011**, *41*, 645–655. [[CrossRef](#)] [[PubMed](#)]
8. Shwab, E.K.; Zhu, X.Q.; Majumdar, D.; Pena, H.F.; Gennari, S.M.; Dubey, J.P.; Su, C. Geographical patterns of *Toxoplasma gondii* genetic diversity revealed by multilocus PCR-RFLP genotyping. *Parasitology* **2014**, *141*, 453–461. [[CrossRef](#)]
9. Minot, S.; Melo, M.B.; Li, F.; Lu, D.; Niedelman, W.; Levine, S.S.; Saeij, J.P. Admixture and recombination among *Toxoplasma gondii* lineages explain global genome diversity. *Proc. Natl. Acad. Sci. USA* **2012**, *109*, 13458–13463. [[CrossRef](#)] [[PubMed](#)]
10. Su, C.; Khan, A.; Zhou, P.; Majumdar, D.; Ajzenberg, D.; Darde, M.L.; Zhu, X.Q.; Ajioka, J.W.; Rosenthal, B.M.; Dubey, J.P.; et al. Globally diverse *Toxoplasma gondii* isolates comprise six major clades originating from a small number of distinct ancestral lineages. *Proc. Natl. Acad. Sci. USA* **2012**, *109*, 5844–5849. [[CrossRef](#)]
11. Glasner, P.D.; Silveira, C.; Kruszon-Moran, D.; Martins, M.C.; Burnier Junior, M.; Silveira, S.; Camargo, M.E.; Nussenblatt, R.B.; Kaslow, R.A.; Belfort Junior, R. An unusually high prevalence of ocular toxoplasmosis in southern Brazil. *Am. J. Ophthalmol.* **1992**, *114*, 136–144. [[CrossRef](#)]
12. De-la-Torre, A.; Gonzalez, G.; Diaz-Ramirez, J.; Gomez-Marin, J.E. Screening by ophthalmoscopy for *Toxoplasma retinochoroiditis* in Colombia. *Am. J. Ophthalmol.* **2007**, *143*, 354–356. [[CrossRef](#)] [[PubMed](#)]
13. Pfaff, A.W.; de-la-Torre, A.; Rochet, E.; Brunet, J.; Sabou, M.; Sauer, A.; Bourcier, T.; Gomez-Marin, J.E.; Candolfi, E. New clinical and experimental insights into Old World and neotropical ocular toxoplasmosis. *Int. J. Parasitol.* **2014**, *44*, 99–107. [[CrossRef](#)] [[PubMed](#)]
14. Reichenbach, A.; Bringmann, A. New functions of Muller cells. *Glia* **2013**, *61*, 651–678. [[CrossRef](#)] [[PubMed](#)]
15. Shamsuddin, N.; Kumar, A. TLR2 mediates the innate response of retinal Muller glia to *Staphylococcus aureus*. *J. Immunol.* **2011**, *186*, 7089–7097. [[CrossRef](#)] [[PubMed](#)]
16. Kumar, A.; Pandey, R.K.; Miller, L.J.; Singh, P.K.; Kanwar, M. Muller glia in retinal innate immunity: A perspective on their roles in endophthalmitis. *Crit. Rev. Immunol.* **2013**, *33*, 119–135. [[CrossRef](#)]
17. Kumar, A.; Shamsuddin, N. Retinal Muller glia initiate innate response to infectious stimuli via toll-like receptor signaling. *PLoS ONE* **2012**, *7*, e29830.
18. Knight, B.C.; Kissane, S.; Falciani, F.; Salmon, M.; Stanford, M.R.; Wallace, G.R. Expression analysis of immune response genes of Muller cells infected with *Toxoplasma gondii*. *J. Neuroimmunol.* **2006**, *179*, 126–131. [[CrossRef](#)]
19. Furtado, J.M.; Ashander, L.M.; Mohs, K.; Chipps, T.J.; Appukuttan, B.; Smith, J.R. *Toxoplasma gondii* migration within and infection of human retina. *PLoS ONE* **2013**, *8*, e54358. [[CrossRef](#)]
20. Lahmar, I.; Guinard, M.; Sauer, A.; Marcellin, L.; Abdelrahman, T.; Roux, M.; Mousli, M.; Moussa, A.; Babba, H.; Pfaff, A.W.; et al. Murine neonatal infection provides an efficient model for congenital ocular toxoplasmosis. *Exp. Parasitol.* **2010**, *124*, 190–196. [[CrossRef](#)]
21. McMenamin, P.G.; Dutton, G.N.; Hay, J.; Cameron, S. The ultrastructural pathology of congenital murine toxoplasmic retinochoroiditis. Part I: The localization and morphology of *Toxoplasma* cysts in the retina. *Exp. Eye Res.* **1986**, *43*, 529–543. [[CrossRef](#)]
22. Pavesio, C.E.; Chiappino, M.L.; Gormley, P.; Setzer, P.Y.; Nichols, B.A. Acquired retinochoroiditis in hamsters inoculated with ME 49 strain *Toxoplasma*. *Invest. Ophthalmol. Vis. Sci.* **1995**, *36*, 2166–2175. [[PubMed](#)]
23. Song, H.B.; Jung, B.K.; Kim, J.H.; Lee, Y.H.; Choi, M.H.; Kim, J.H. Investigation of tissue cysts in the retina in a mouse model of ocular toxoplasmosis: Distribution and interaction with glial cells. *Parasitol. Res.* **2018**, *117*, 2597–2605. [[CrossRef](#)] [[PubMed](#)]
24. Sun, M.; Kraus, W.L. From discovery to function: The expanding roles of long noncoding RNAs in physiology and disease. *Endocr. Rev.* **2015**, *36*, 25–64. [[CrossRef](#)] [[PubMed](#)]
25. Choi, S.W.; Kim, H.W.; Nam, J.W. The small peptide world in long noncoding RNAs. *Brief Bioinform.* **2018**. [[CrossRef](#)] [[PubMed](#)]

26. Dhir, A.; Dhir, S.; Proudfoot, N.J.; Jopling, C.L. Microprocessor mediates transcriptional termination of long noncoding RNA transcripts hosting microRNAs. *Nat. Struct. Mol. Biol.* **2015**, *22*, 319–327. [[CrossRef](#)] [[PubMed](#)]
27. Hadjicharalambous, M.R.; Lindsay, M.A. Long non-coding RNAs and the innate immune response. *Noncoding RNA* **2019**, *5*, 34. [[CrossRef](#)] [[PubMed](#)]
28. Agliano, F.; Rathinam, V.A.; Medvedev, A.E.; Vanaja, S.K.; Vella, A.T. Long noncoding RNAs in host-pathogen interactions. *Trends Immunol.* **2019**, *40*, 492–510. [[CrossRef](#)]
29. Chen, Y.G.; Satpathy, A.T.; Chang, H.Y. Gene regulation in the immune system by long noncoding RNAs. *Nat. Immunol.* **2017**, *18*, 962–972. [[CrossRef](#)]
30. Fernandes, J.C.R.; Acuna, S.M.; Aoki, J.I.; Floeter-Winter, L.M.; Muxel, S.M. Long non-coding RNAs in the regulation of gene expression: Physiology and disease. *Noncoding RNA* **2019**, *5*, 17. [[CrossRef](#)]
31. Mumtaz, P.T.; Bhat, S.A.; Ahmad, S.M.; Dar, M.A.; Ahmed, R.; Urwat, U.; Ayaz, A.; Shrivastava, D.; Shah, R.A.; Ganai, N.A. LncRNAs and immunity: Watchdogs for host pathogen interactions. *Biol. Proced. Online* **2017**, *19*, 3. [[CrossRef](#)] [[PubMed](#)]
32. Mathy, N.W.; Chen, X.M. Long non-coding RNAs (lncRNAs) and their transcriptional control of inflammatory responses. *J. Biol. Chem.* **2017**, *292*, 12375–12382. [[CrossRef](#)] [[PubMed](#)]
33. Zhang, Y.; Cao, X. Long noncoding RNAs in innate immunity. *Cell. Mol. Immunol.* **2016**, *13*, 138–147. [[CrossRef](#)] [[PubMed](#)]
34. Gomez, J.A.; Wapinski, O.L.; Yang, Y.W.; Bureau, J.F.; Gopinath, S.; Monack, D.M.; Chang, H.Y.; Brahic, M.; Kirkegaard, K. The NeST long ncRNA controls microbial susceptibility and epigenetic activation of the interferon-gamma locus. *Cell* **2013**, *152*, 743–754. [[CrossRef](#)] [[PubMed](#)]
35. Li, J.; Chen, C.; Ma, X.; Geng, G.; Liu, B.; Zhang, Y.; Zhang, S.; Zhong, F.; Liu, C.; Yin, Y.; et al. Long noncoding RNA NRON contributes to HIV-1 latency by specifically inducing tat protein degradation. *Nat. Commun.* **2016**, *7*, 11730. [[CrossRef](#)] [[PubMed](#)]
36. Lahmar, I.; Pfaff, A.W.; Marcellin, L.; Sauer, A.; Moussa, A.; Babba, H.; Candolfi, E. Muller cell activation and photoreceptor depletion in a mice model of congenital ocular toxoplasmosis. *Exp. Parasitol.* **2014**, *144*, 22–26. [[CrossRef](#)] [[PubMed](#)]
37. Liu, W.; Huang, L.; Wei, Q.; Zhang, Y.; Zhang, S.; Zhang, W.; Cai, L.; Liang, S. Microarray analysis of long non-coding RNA expression profiles uncovers a *Toxoplasma*-induced negative regulation of host immune signaling. *Parasit. Vectors* **2018**, *11*, 174. [[CrossRef](#)]
38. Menard, K.L.; Haskins, B.E.; Colombo, A.P.; Denkers, E.Y. *Toxoplasma gondii* manipulates expression of host long noncoding RNA during intracellular infection. *Sci. Rep.* **2018**, *8*, 15017. [[CrossRef](#)]
39. Guttman, M.; Amit, I.; Garber, M.; French, C.; Lin, M.F.; Feldser, D.; Huarte, M.; Zuk, O.; Carey, B.W.; Cassady, J.P.; et al. Chromatin signature reveals over a thousand highly conserved large non-coding RNAs in mammals. *Nature* **2009**, *458*, 223–227. [[CrossRef](#)]
40. Suzuki, Y.; Orellana, M.A.; Schreiber, R.D.; Remington, J.S. Interferon-gamma: The major mediator of resistance against *Toxoplasma gondii*. *Science* **1988**, *240*, 516–518. [[CrossRef](#)]
41. Castro, F.; Cardoso, A.P.; Gonçalves, R.M.; Serre, K.; Oliveira, M.J. Interferon-gamma at the crossroads of tumor immune surveillance or evasion. *Front. Immunol.* **2018**, *9*, 847. [[CrossRef](#)]
42. Spurlock, C.F., 3rd; Croke, P.S., 3rd; Aune, T.M. Biogenesis and transcriptional regulation of long noncoding RNAs in the human immune system. *J. Immunol.* **2016**, *197*, 4509–4517. [[CrossRef](#)] [[PubMed](#)]
43. Kuo, G.; Wu, C.Y.; Yang, H.Y. MiR-17-92 cluster and immunity. *J. Formos. Med. Assoc.* **2019**, *118*, 2–6. [[CrossRef](#)] [[PubMed](#)]
44. Yao, Y.; Jiang, Q.; Jiang, L.; Wu, J.; Zhang, Q.; Wang, J.; Feng, H.; Zang, P. Lnc-SGK1 induced by *Helicobacter pylori* infection and high salt diet promote Th2 and Th17 differentiation in human gastric cancer by SGK1/Jun B signaling. *Oncotarget* **2016**, *7*, 20549–20560. [[CrossRef](#)] [[PubMed](#)]
45. Li, J.Q.; Hu, S.Y.; Wang, Z.Y.; Lin, J.; Jian, S.; Dong, Y.C.; Wu, X.F.; Dai, L.; Cao, L.J. Long non-coding RNA MEG3 inhibits microRNA-125a-5p expression and induces immune imbalance of Treg/Th17 in immune thrombocytopenic purpura. *Biomed. Pharm.* **2016**, *83*, 905–911. [[CrossRef](#)] [[PubMed](#)]
46. Qiu, Y.Y.; Wu, Y.; Lin, M.J.; Bian, T.; Xiao, Y.L.; Qin, C. LncRNA-MEG3 functions as a competing endogenous RNA to regulate Treg/Th17 balance in patients with asthma by targeting microRNA-17/ RORgammat. *Biomed. Pharm.* **2019**, *111*, 386–394. [[CrossRef](#)] [[PubMed](#)]

47. Lahmar, I.; Abou-Bacar, A.; Abdelrahman, T.; Guinard, M.; Babba, H.; Ben Yahia, S.; Kairallah, M.; Speeg-Schatz, C.; Bourcier, T.; Sauer, A.; et al. Cytokine profiles in toxoplasmic and viral uveitis. *J. Infect. Dis.* **2009**, *199*, 1239–1249. [[CrossRef](#)]
48. Sauer, A.; Pfaff, A.W.; Villard, O.; Creuzot-Garcher, C.; Dalle, F.; Chiquet, C.; Pelloux, H.; Speeg-Schatz, C.; Gaucher, D.; Prevost, G.; et al. Interleukin 17A as an effective target for anti-inflammatory and antiparasitic treatment of toxoplasmic uveitis. *J. Infect. Dis.* **2012**, *206*, 1319–1329. [[CrossRef](#)]
49. Sherrill, J.D.; Kiran, K.C.; Blanchard, C.; Stucke, E.M.; Kemme, K.A.; Collins, M.H.; Abonia, J.P.; Putnam, P.E.; Mukkada, V.A.; Kaul, A.; et al. Analysis and expansion of the eosinophilic esophagitis transcriptome by RNA sequencing. *Genes Immun.* **2014**, *15*, 361–369. [[CrossRef](#)]
50. Li, D.Y.; Chen, W.J.; Shang, J.; Chen, G.; Li, S.K. Regulatory interactions between long noncoding RNA LINC00968 and miR-9-3p in non-small cell lung cancer: A bioinformatic analysis based on miRNA microarray, GEO and TCGA. *Oncol. Lett.* **2018**, *15*, 9487–9497. [[CrossRef](#)]
51. Wang, Y.; Zhou, J.; Xu, Y.J.; Hu, H.B. Long non-coding RNA LINC00968 acts as oncogene in NSCLC by activating the Wnt signaling pathway. *J. Cell. Physiol.* **2018**, *233*, 3397–3406. [[CrossRef](#)] [[PubMed](#)]
52. Li, Z.; Yu, Z.; Meng, X.; Yu, P. LncRNA LINC00968 accelerates the proliferation and fibrosis of diabetic nephropathy by epigenetically repressing p21 via recruiting EZH2. *Biochem. Biophys. Res. Commun.* **2018**, *504*, 499–504. [[CrossRef](#)] [[PubMed](#)]
53. Li, R.; Zhang, L.; Jia, L.; Duan, Y.; Li, Y.; Bao, L.; Sha, N. Long non-coding RNA BANCR promotes proliferation in malignant melanoma by regulating MAPK pathway activation. *PLoS ONE* **2014**, *9*, e100893. [[CrossRef](#)] [[PubMed](#)]
54. Jiang, W.; Zhang, D.; Xu, B.; Wu, Z.; Liu, S.; Zhang, L.; Tian, Y.; Han, X.; Tian, D. Long non-coding RNA BANCR promotes proliferation and migration of lung carcinoma via MAPK pathways. *Biomed. Pharm.* **2015**, *69*, 90–95. [[CrossRef](#)] [[PubMed](#)]
55. Loewer, S.; Cabili, M.N.; Guttman, M.; Loh, Y.H.; Thomas, K.; Park, I.H.; Garber, M.; Curran, M.; Onder, T.; Agarwal, S.; et al. Large intergenic non-coding RNA-RoR modulates reprogramming of human induced pluripotent stem cells. *Nat. Genet.* **2010**, *42*, 1113–1117. [[CrossRef](#)] [[PubMed](#)]
56. Zhang, A.; Zhou, N.; Huang, J.; Liu, Q.; Fukuda, K.; Ma, D.; Lu, Z.; Bai, C.; Watabe, K.; Mo, Y.Y. The human long non-coding RNA-RoR is a p53 repressor in response to DNA damage. *Cell Res.* **2013**, *23*, 340–350. [[CrossRef](#)]
57. Brunet, J.; Pfaff, A.W.; Abidi, A.; Unoki, M.; Nakamura, Y.; Guinard, M.; Klein, J.P.; Candolfi, E.; Mousli, M. *Toxoplasma gondii* exploits UHRF1 and induces host cell cycle arrest at G2 to enable its proliferation. *Cell. Microbiol.* **2008**, *10*, 908–920. [[CrossRef](#)]
58. Molestina, R.E.; El-Guendy, N.; Sinai, A.P. Infection with *Toxoplasma gondii* results in dysregulation of the host cell cycle. *Cell. Microbiol.* **2008**, *10*, 1153–1165. [[CrossRef](#)]
59. Angeloni, M.B.; Silva, N.M.; Castro, A.S.; Gomes, A.O.; Silva, D.A.; Mineo, J.R.; Ferro, E.A. Apoptosis and S phase of the cell cycle in BeWo trophoblastic and HeLa cells are differentially modulated by *Toxoplasma gondii* strain types. *Placenta* **2009**, *30*, 785–791. [[CrossRef](#)]
60. Lavine, M.D.; Arrizabalaga, G. Induction of mitotic S-phase of host and neighboring cells by *Toxoplasma gondii* enhances parasite invasion. *Mol. Biochem. Parasitol.* **2009**, *164*, 95–99. [[CrossRef](#)]
61. Wang, G.; Gao, M. Influence of *Toxoplasma gondii* on in vitro proliferation and apoptosis of hepatoma carcinoma H7402 cell. *Asian Pac. J. Trop. Med.* **2016**, *9*, 63–66. [[CrossRef](#)] [[PubMed](#)]
62. Limb, G.A.; Salt, T.E.; Munro, P.M.; Moss, S.E.; Khaw, P.T. In vitro characterization of a spontaneously immortalized human Muller cell line (MIO-M1). *Invest. Ophthalmol. Vis. Sci.* **2002**, *43*, 864–869. [[PubMed](#)]
63. Sibley, L.D.; Boothroyd, J.C. Virulent strains of *Toxoplasma gondii* comprise a single clonal lineage. *Nature* **1992**, *359*, 82–85. [[CrossRef](#)] [[PubMed](#)]
64. Khan, A.; Fux, B.; Su, C.; Dubey, J.P.; Darde, M.L.; Ajioka, J.W.; Rosenthal, B.M.; Sibley, L.D. Recent transcontinental sweep of *Toxoplasma gondii* driven by a single monomorphic chromosome. *Proc. Natl. Acad. Sci. USA* **2007**, *104*, 14872–14877. [[CrossRef](#)] [[PubMed](#)]
65. Khan, A.; Behnke, M.S.; Dunay, I.R.; White, M.W.; Sibley, L.D. Phenotypic and gene expression changes among clonal type I strains of *Toxoplasma gondii*. *Eukaryot. Cell* **2009**, *8*, 1828–1836. [[CrossRef](#)] [[PubMed](#)]
66. Pfaffl, M.W. A new mathematical model for relative quantification in real-time RT-PCR. *Nucleic Acids Res.* **2001**, *29*, e45. [[CrossRef](#)] [[PubMed](#)]

67. Helleman, J.; Mortier, G.; De Paepe, A.; Speleman, F.; Vandesompele, J. qBase relative quantification framework and software for management and automated analysis of real-time quantitative PCR data. *Genome Biol.* **2007**, *8*, R19. [[CrossRef](#)]
68. Appukuttan, B.; Ashander, L.M.; Ma, Y.; Smith, J.R. Selection of reference genes for studies of human retinal endothelial cell gene expression by reverse transcription-quantitative real-time polymerase chain reaction. *Gene Rep.* **2018**, *10*, 123–134. [[CrossRef](#)]



© 2019 by the authors. Licensee MDPI, Basel, Switzerland. This article is an open access article distributed under the terms and conditions of the Creative Commons Attribution (CC BY) license (<http://creativecommons.org/licenses/by/4.0/>).